 DOI: 10.1002/masy.200950701

Heterophase Polymerization as Synthetic Tool in Polymer Chemistry for Making Nanocomposites

Klaus Tauer, Nancy Weber, Samira Nozari, Klaus Padtberg, Reinhard Sigel, Arne Stark, Antje Völkel*

Summary: The paper considers various possibilities to produce inorganic – polymeric nanocomposites via aqueous heterophase polymerization. Special emphasis is placed on strategies to synthesize nanocomposite particles via joint nucleation or joint polymerization. The former strategy is used to make composite particles with $CaCO_3$ as inorganic component. The strategy of joint polymerization takes advantage from the condition that aqueous heterophase polymerization is a convenient possibility to synthesize amphiphilic block copolymers. This method relies on the fact that polymeric radicals can survive in isolated latex particles that are stabilized by hydrophilic blocks. This strategy can be successfully applied to produce silica-containing block copolymer particles in a one-step procedure.

Keywords: block copolymers; calcium carbonate; heterophase polymerization; nano-composites; silica

Introduction

In general, there exist three different strategies for the synthesis of binary composite latex particles of inorganic and polymeric materials. First, one preformed component is employed during the generation of the other, second, both components are generated during the same reaction in-situ either simultaneously or consecutively by sequential addition of the educts, and third, two preformed components are employed to form the nanocomposite particles. The most prominent process of making composite nanoparticles via heterophase polymerization is the encapsulation of preformed inorganic particles as recently reviewed in ref.[1,2]. To start the generation of inorganic particles in the presence of preformed polymers, that is the Nature's route of making bones and teeth, is also known as biomineralization and intensively studied.[3–6] Two examples which take advantage of the application of block copolymers made by heterophase polymerization are the formation of helical barium carbonate fibers in the presence of poly(ethylene glycol)-*block*-{(2-(4-dihydroxyphosphoryl)-2-oxabutyl) acrylate ethylester}[7] and the synthesis of aragonite superstructures templated by double hydrophilic triblock copolymer particles, poly[2-(diethylamino)ethyl methacrylate]-*block*-poly(*N*-isopropylacrylamide)-*block*-poly (methacrylic acid) in which the poly (methacrylic acid) core is cross-linked with 1,3-diisopropenylbenzene.[8]

This contribution deals in more detail with the other options that is, (1) in-situ and simultaneous generation of both components and (2) combination of the two preformed materials.

Experimental Part

Water was taken from a Seral purification system (PURELAB Plus) with a conductivity of 0.06 $\mu S\ cm^{-1}$ which was degassed prior to use for the nucleation experiments. Styrene, butyl acrylate (BuA), and butyl methacrylate (BuMA) (all from Aldrich)

Max Planck Institute of Colloids and Interfaces, Am Mühlenberg, D-14476 Golm, Germany
E-mail: klaus.tauer@mpikg.mpg.de

were distilled under reduced pressure to remove inhibitors. Potassium peroxodisulfate (KPS, Sigma Aldrich), vinyl trimethoxysilane (VTMeOS, Aldrich), methyl trimethoxysilane (MTMeOS, ABCR), vinyl trimethylsilane (VTMeS, ABCR), tetramethylsilane (TeMS, Acros), poly(ethylene glycol) with different molecular weight (PEG, Aldrich or Fluka), methoxy-terminated PEG with a molecular weight of 5000 g/mol (mPEG5000, Aldrich), and Ludox silica particles (Aldrich) were all used as received. The polystyrene (PS) latex EUR63 was prepared by batch emulsion polymerization (40 g of water, 10 g of styrene, 80 °C) with sodium perfluorooctanoate (0.04 g) as emulsifier and a poly(ethylene glycol) azo initiator (0.673 g, PEGA200 [9]). The methods for carrying out the joint nucleation experiments are described in.[10,11] The procedure used for the preparation of block copolymers via heterophase polymerization is described elsewhere.[12] For the results reported here the following general recipe and procedure was used. All block copolymers were synthesized in a CPA200 reaction calorimeter (ChemiSens AB, Lund, Sweden). The water soluble precursor polymer (2.1 g mPEG5000) and 3.16 g *N*-isopropylacrylamide (NIPAM) were dissolved in 90 g H_2O and equilibrated at the polymerization temperature 60 °C. The polymerization was started by adding 0,4 g ceric ammonium nitrate dissolved in 10 g of 1 M HNO_3. After the NIPAM polymerization was complete the Si-monomer was added. Before any analysis the final latexes were purified by ultrafiltration through a YM-100 membrane (regenerated cellulose) with a cut-off of 100 kDa until the conductivity of the eluate reached a constant values. Then, the block copolymers were isolated by freeze-drying (Beta 1–16, Christ, Germany). FT-IR spectra were recorded with a Varian 1000 Scimitar in ATR mode (Pike Miracle ATR cell). Transmission and scanning electron microscopy (TEM, SEM) was performed with a Zeiss EM 912 Omega microscope operating at 100 kV and a Leo Gemini 1550 according to standard procedures, respectively. The particle size and density distribution measurements of the PMMA – $CaCO_3$ composite particles were carried out with an analytical ultracentrifuge, Beckman Optima^{TM} XL-80K with 633 nm laser on a fixed location in H_2O and D_2O mixtures and evaluated according to standard procedures.[13]

Results and Discussion

Simultaneous Generation of both Components – 1. Joint Nucleation

Joint nucleation, that is the simultaneous in-situ formation of the inorganic and polymeric material under heterophase polymerization conditions, appeared as an attractive possibility to generate nanoscale composite materials. Based on studies on particle nucleation in both emulsion polymerization and precipitation of inorganic salts[11] conditions have been determined so that the nucleation of inorganic and polymeric particles can take place simultaneously. The protocol of such a reaction is depicted in Figure 1 illustrating the

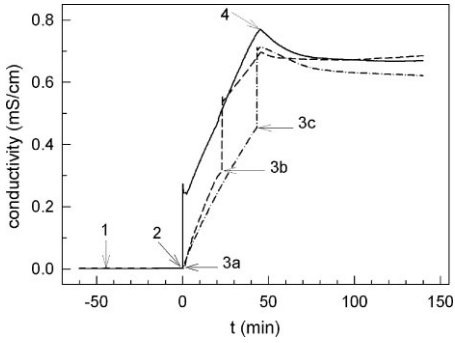

Figure 1.
Conductivity change during the joint nucleation of $CaCO_3$ and polystyrene particles;[14] 1 – styrene (5 g) is placed on the top of 390 g of water; thermal equilibration to 70 °C; 2 – start separate feeding (1 ml/h) of 0.5 M $CaCl_2$ and 0.5 M Na_2CO_3 solutions with syringe pumps; 3 – addition of 10 ml of 20 mM KPS solution a – simultaneously with, b – 23 minutes after, and c – 45 minutes after the start of feeding of calcium chloride and sodium carbonate; 4 – stop feeding of $CaCl_2$ and Na_2CO_3.

preparation of calcium carbonate – polystyrene nanocomposites. The all-Teflon reactor is equipped with a conductivity probe and a vis-spectrometer, thus allowing on-line measurements of the conductivity and the turbidity of the aqueous reaction mixture.

Comparison experiments in the presence of styrene but without KPS show that the time when formation of calcium carbonate particles is observed scatters between $t = 15$–60 min. As the solubility of $CaCO_3$ is reached after about 10–12 minutes a lag-time ranging from a couple of minutes to 45 minutes underlines the inherent scatter of this nucleation process. The time it takes after KPS addition until the nucleation in styrene emulsion polymerization takes place, without addition of calcium chloride/sodium carbonate, scatters between 20 and 30 minutes. The nucleation event is in either separate case indicated by a distinct bend in the conductivity – time curve.[10,15] During the joint nucleation experiments the conductivity – time curve is governed by the feeding of the salt solutions and only after stopping the feed, reactions leading to a change in the conductivity become influential. For the reaction depicted in Figure 1 the joint nucleation is controlled by the time when the polymerization is started. The TEM images of Figure 2 show that it is indeed possible to influence the morphology of the particles by adjusting the duration of the pre-nucleation period in which the supersaturation builds up. Due to the above mentioned difficulties to identify the onset of the nucleation it is not possible to conclude clearly to what extent both nucleation processes concomitantly influence each other.

Images 2C and 2D clearly show polystyrene – $CaCO_3$ composite latex particles. Due to the higher electron density the tiny dark regions inside the larger particles represent $CaCO_3$ domains. Obviously, the joint nucleation of such nanocomposites is possible as long as the supersaturation for both nucleation events is built up simultaneously corresponding to the experimental conditions 3a and 3b of Figure 1. Image 2E

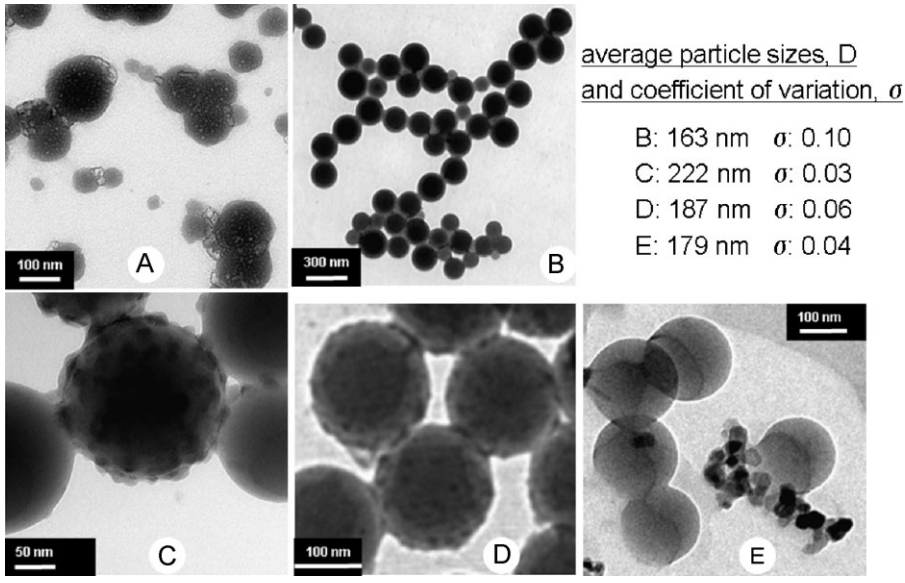

Figure 2.
TEM images A and B show nanoparticles of calcium carbonate and polystyrene, respectively, prepared in separate comparison experiments; images C, D, and E show nanoparticles as obtained in the joint nucleation experiments when KPS addition was started together with (C), after 23 minutes (D) and 45 minutes after beginning of the $CaCl_2/Na_2CO_3$ feed, respectively (cf. caption of Figure 1 for experimental conditions).

as obtained when KPS was added after the salt feed was stopped (condition 3c of Figure 1) shows separately nucleated $CaCO_3$ (smaller darker particles) and polystyrene particles. The average particle sizes (the table in the upper right corner of Figure 2) determined by enumerating the corresponding TEM images show that, firstly, the composite particles are expectedly of larger size than the neat polystyrene particles and, secondly, the increasing ionic strength in the reaction system increases the average particle size (cf. A and E) and reduces slightly the width of the particle size distribution. The data put together in Figure 3 prove that the procedure of joint nucleation can also be applied to produce poly(methyl methacrylate) (PMMA) – $CaCO_3$ composite particles. In cases where TEM images are not able to prove visually the formation of composite particles analytical ultracentrifugation (AUC) is a very useful technique (Figure 3E). The average particle density as determined by AUC increases with increasing particle size and indicates a higher content of $CaCO_3$ in larger particles. Again, also in this case the composite particles are of larger size than the neat PMMA particles.

In contrast to polystyrene the PMMA composite nanoparticles of images 3B, 3C, and 3D exhibit core – shell morphology which is clearly indicated by the darker edges of the composite particles. The mineral shell prevents that the composite PMMA particles flow together under the electron beam like it is the case for the neat PMMA particles (3A). Image 3B shows not only spherical composite particles but also calcium carbonate needles as it should be the case under these particular experimental conditions (start of the

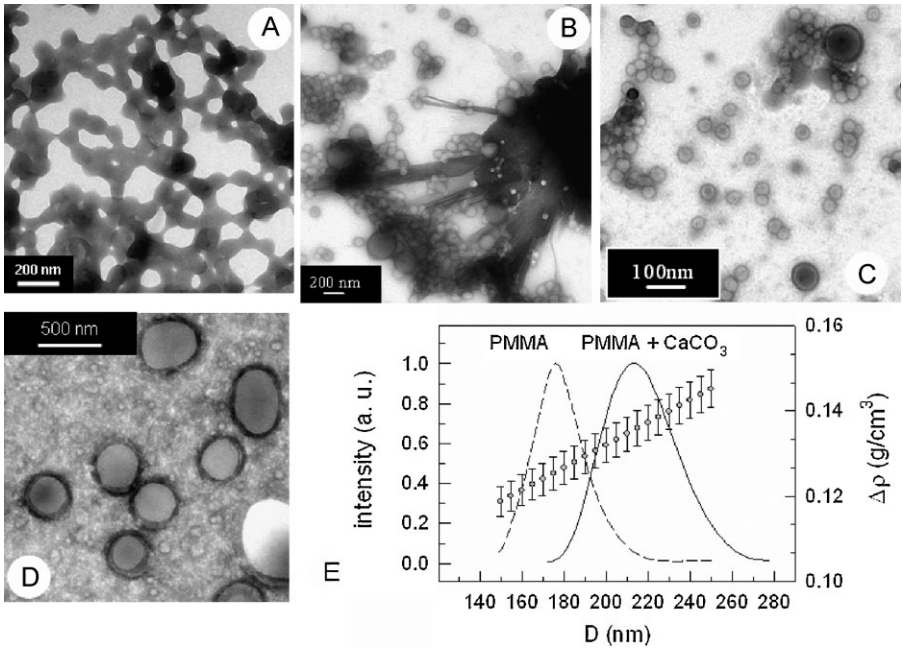

Figure 3.
TEM image of neat PMMA comparison particles (A) and of PMMA – $CaCO_3$ composite particles (B, C, D); recipe: 5 g of MMA, KPS concentration 0,1 mM, temperature 70 °C, 0.5 M $CaCl_2$ and Na_2CO_3 solution feed with 1 ml/h over a duration of 200 minutes; image B and C represent joint nucleation experiments where the polymerization was started by KPS addition after nucleation of $CaCO_3$ (132 minutes after starting the salt feed)[16]; image D corresponds to a joint nucleation experiment where the salt feed was stopped after 60 minutes and KPS was added before the nucleation of $CaCO_3$ crystals could be detected; polymerization conditions for the data of image E correspond to these for image B except that KPS was added in the middle of the salt feed.[14]

polymerization after $CaCO_3$ nucleation and continuation of salt feed for 30 minutes). These needles are aragonite which is the $CaCO_3$ modification formed at higher temperatures.[16] Under the conditions of experiment D $CaCO_3$ particles have not been formed before the polymerization was started and hence, aragonite needles could not been detected. The formation of PMMA – $CaCO_3$ core - shell particles allows conclusions regarding the mechanism of the joint nucleation: PMMA particles are generated, possibly facilitated by the high ionic strength due to the salt feed, before $CaCO_3$ particles are formed via heterogeneous nucleation at the polymer water interface.

These investigations prove that joint nucleation experiments lead to composite nanoparticles. The morphology of $CaCO_3$ in the composite particles depends on the nature of the polymer component and can be either shell-like (PMMA) or dispersion-like (PS).

Simultaneous Generation of both Components – 2. Joint Polymerization

Joint polymerization means the application of two different polymerization mechanisms in a single heterophase polymerization reaction carried out in the way suited to synthesize block copolymers.[12,17–19] This particular route to prepare block copolymers via radical heterophase polymerization is easy and versatile. It utilizes polymeric primary free radicals formed via the redox reaction between ceric ions and methylol endgroups of hydrophilic precursor polymers and subsequently sequential addition of monomers. This procedure fulfils all requirements for the formation of block copolymers, which are firstly a short period of the formation of the growing species (radicals),[18] secondly a low probability of termination as only polymeric radicals are involved, and thirdly the sequential monomer addition. Moreover, the formation of block copolymers is facilitated inside the polymeric particles formed in the course of the reaction as NIPAM is the first monomer and the polymerization temperature is above the lower critical solution temperature of PNIPAM. After the NIPAM polymerization is completed a second monomer is added. The sequential polymerizations can easily be followed in a reaction calorimeter and the success of the block copolymer formation is immediately visible if, for a hydrophobic second-stage monomer, the reaction mixture is after completion of the polymerization still a stable dispersion at room temperature. A typical calorimetric record of such a polymerization is shown in Figure 4 together with a summary of the precursor polymers and monomers employed. The result of the polymerization illustrated by the calorimetric curve of Figure 4 is a PEG-PNIPAM-PVTMeOS triblock copolymer dispersion that is stable also at room temperature. After ultrafiltration and freeze-drying the solid triblock copolymer is easily redispersable in water. TEM images (Figure 5A) clearly show regions of higher electron density which suggests the presence of siloxane (SiO_2) units. After calcination pure siloxane particles remain (Figure 5B) and the treatment of the solid triblock copolymer in a high temperature flame leads to macroscopic quartz pearls (Figure 5C). Besides this preparative proofs of the triblock copolymer morphology FT-IR measurements support the structure as sketched in Figure 5D.

The vibration spectrum of the triblock copolymer unambiguously shows, besides the characteristic bands of the PNIPAM and the PEG blocks, the existence of SiO_2 units already in the triblock copolymer (Figure 5E).

These block copolymers have a very special morphology as the double hydrophilic block copolymers are attached to cross-linked silica regions. Obviously, during the polymerization of the VTMeOS monomer radical polymerization and hydrolytic condensation take place simultaneously leading to the structure as sketched in Figure 5D. The strong heat developed after addition of the VTMeOS monomer (cf. Figure 4) is due to the

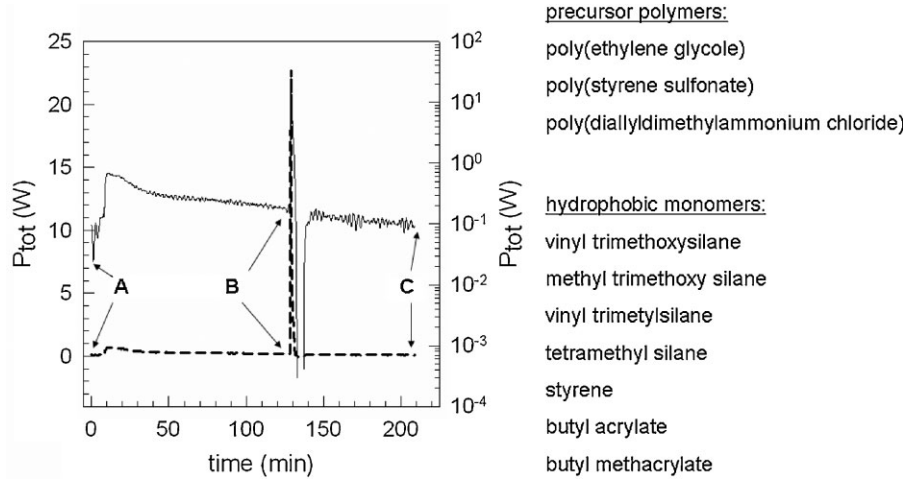

Figure 4.
Calorimetric record of block copolymer formation via heterophase polymerization, total power (P_{tot}) versus time plot (dashed line left Y-axis, solid line logarithmic plot right Y-axis); until A thermal equilibration of water containing the precursor polymer and NIPAM, at A – start of NIPAM polymerization by the addition of ceric ammonium nitrate; B – addition of the second monomer; C – end of the polymerization; recipe: 2,1 g methoxy terminated PEG with a molecular weight of 5000 g/mol; 3,16 g NIPAM in 90 g H_2O; 60 °C; at A: 0,4 g CAN in 10 g HNO_3 (1 M); at B: 4,44 g VTMeOS.

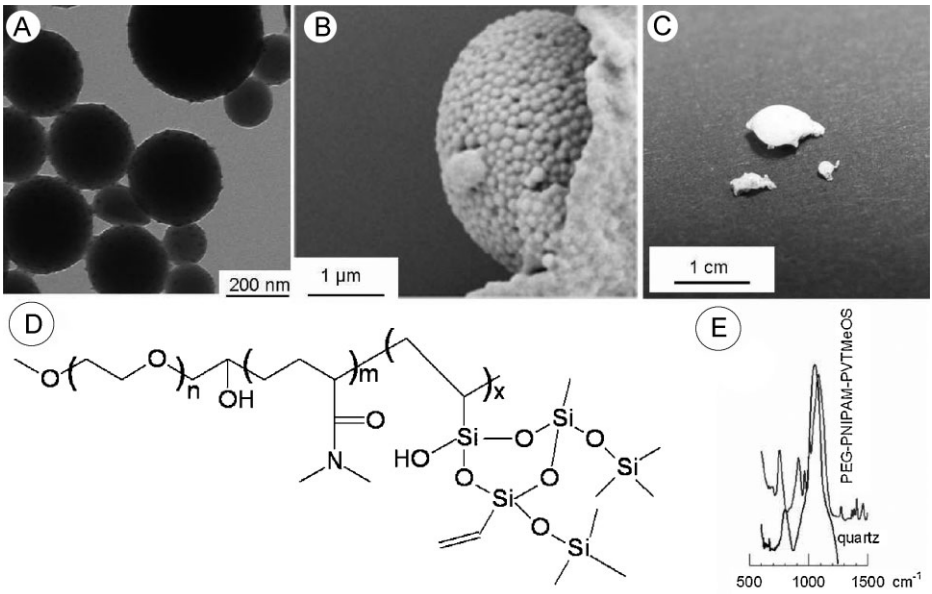

Figure 5.
Images of various states of the PEG-PNIPAM-PVTMeOS triblock copolymer: A – TEM image of the redispersed polymer after ultrafiltration and freeze-drying, B – SEM images of the remaining particles after calcinations for 7 hours at 550 °C; C – quartz pearls after burning the solid polymer in a high-temperature gas flame at 1500 °C; D – sketch of the chemical structure of the PEG-PNIPAM-PVTMeOS triblock copolymer; part of the FT-IR spectra of quartz and the PEG-PNIPAM-PVTMeOS triblock copolymer in the absorption region of the SiO_2 groups.

vigorous reaction with water leading to hydrolysis and subsequent polycondensation.

The crucial point during the block copolymer formation is after the precipitation step when the radicals must survive inside the particles in order to initiate the growth of the next block. The survival of the radicals requires an optimum hydrophilic – hydrophobic balance of the diblock copolymers made of the precursor polymer and the PNIPAM at temperatures above the LCST of PNIPAM. The aggregation power of PNIPAM is strong as above 35 °C also diblock copolymers with long chains of PSS (500–8000 repeat units) and PDADMAC (60–1500 repeat units) as hydrophilic blocks precipitate if they are attached to PNIPAM with chain length between 2500–40.000.[19] Aggregating PNIPAM units can facilitate the encounter of growing radicals and hence, make termination easier possible. The counteracting force arises from the hydrophilicity of the precursor polymer that drives the radical ends apart. An optimum hydrophobic – hydrophilic force balance fixes the diblock copolymer chains in place and reduces radical termination. A systematic variation of the PEG chain length revealed that triblock copolymer formation takes place with VTMeOS and styrene if the PEG chain length is above 2000 and 3000 g/mol, respectively.

Interestingly, if instead of VTMeOS, MTMeOS is used that is only able to polymerize via hydrolytic condensation also stable dispersions are formed. In contrast, VTMS and TeMS do not form stable dispersions although VTMS is able to participate in propagation reaction. These experimental facts allow conclusions regarding the mechanism of the incorporation of the silicium compounds. That MTMeOS leads to stable dispersions points to the importance of chains transfer to the methyl groups as only the hydrolytic condensation is not sufficient to cause block copolymer formation. Figure 6 shows the morphology of the corresponding composite particles after ultrafiltration, freeze

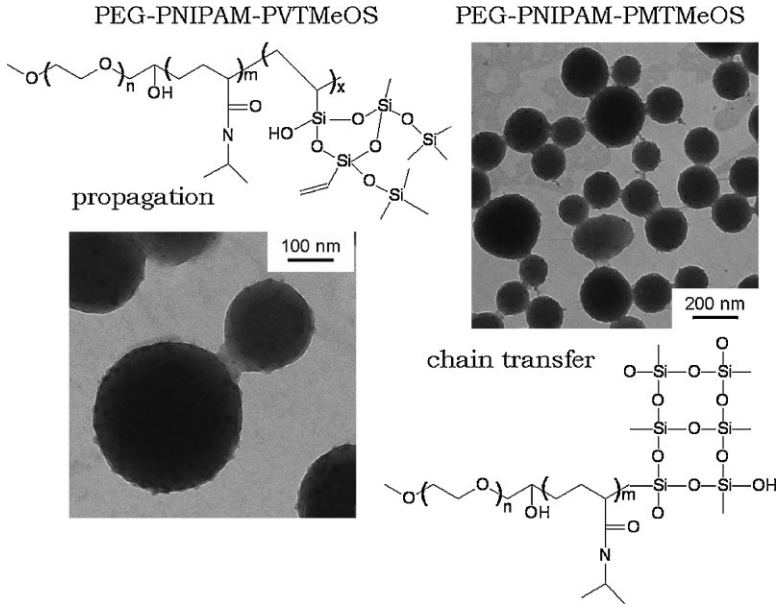

Figure 6.
TEM images of triblock copolymer composite particles after ultrafiltration, freeze-drying, and redispersion and the corresponding chemical structures of PEG-PNIPAM-PVTMeOS (left-hand side) and PEG-PNIPAM-PMTMeOS (right-hand side); PEG is monomethoxy terminated, with a molecular weight of 5000.

drying, and redispersion. In both cases silica nanoparticles are embedded in a less dense polymer structure.

On the other hand, also radical polymerization alone, either propagation or chain transfer, is not enough to cause block copolymer formation as proven by the results obtained with VTMS and TeMS.

An important role in this particular block copolymer formation mechanism plays NIPAM in at least two ways. Firstly, the PNIPM block generates the heterogeneous reaction loci for the polymerization of the hydrophobic monomers and secondly, it ensures that the hydrolytic condensation can take place as PNIPAM above the LCST contains still about 30 wt. % of water.[20,21] In this line, if as second-stage monomer styrene, VTMeOS, or MTMeOs is used dispersions and triblock copolymers are obtained only if a PNIPAM middle block is present. In the absence of the PNIPAM middle block hydrolytic condensation takes place but not the formation of block copolymers.

The morphology of the SiO_2 that is obtained after calcinations depends on the morphology and composition of the block copolymer particles (cf. Figure 5B and Figure 7). Triblock copolymers with PNIPAM middle blocks lead, regardless of the nature of the hydrophilic precursor polymer, to spherical silica particles (image B of Figure 5 and images A and B of Figure 7). If, however, the core of the block copolymer particles consists of a hydrophobic polymer such as BuA or BuMA the morphology of the silica after calcination changes completely as a macroscopic solid with nanopores is obtained (cf. images C and D of Figure 7).

The images put together in Figure 7 support the idea that the hydrolytic condensation takes place inside the region

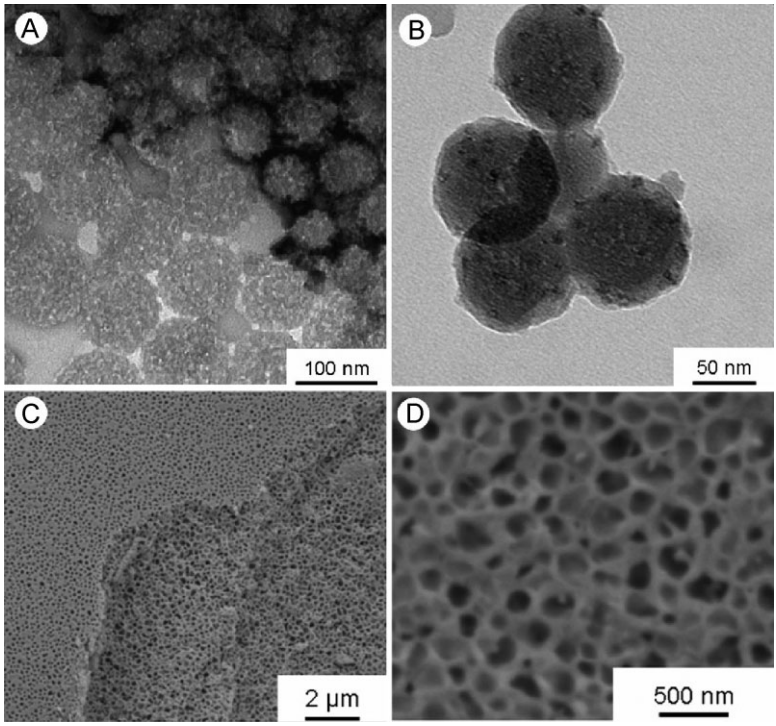

Figure 7.
TEM (A, B) and SEM (C, D) images of the silica obtained after calcination of various block copolymer particles; A - PSS-PNIPAM-PVTMeOS (after washing the solid with water[22]); B - PDADMAC-PNIPAM-PVTMeOS; C - PEG-PNIPAM-PBuA-PVTMeOS; D - PEG-PNIPAM-PBuMA-PMTMeOS.

where the PNIPAM block is located. This is for the triblock copolymers (PSS-PNIPAM-PVTMeOS, PDADMAC-PNIPAM-PVTMeOS) the core of the particles and for the PEG-PNIPAM-PBuA-PVTMeOS and PEG-PNIPAM-PBuMA-PMTMeOS multiblock copolymers a region around the hydrophobic PBuA and PBuMA cores, respectively. Assuming such block copolymer morphologies explains convincingly the formation of silica nanoparticles and nanoporous silica.

Combination of Two Preformed Materials to Create Nanocomposites

The combination of two preformed materials to create inorganic – polymeric nanocomposites, as discussed in this part, requires the application of inorganic colloids and utilizes the effect that is called spontaneous emulsification.[23,24] Spontaneous emulsification describes the experimental finding that any combination of immiscible liquids leads to the spontaneous formation of an emulsion on either side of the interface without any input of mechanical energy, that is, at the quiescent interface. For instance, a few minutes after placing very carefully styrene on water, water droplets on the styrene side and styrene drops on the water side can be observed with a light microscope working in an ultramicroscope - like fashion.[23] If instead of the pure organic liquid a solution is put on the top of water containing polymer particles spontaneous emulsification causes a variety of effects depending on the nature of the materials involved. If the organic liquid that is a solvent for the polymer contains a hydrophobic dye such as Sudan IV, Solvent Blue, or Hostasol Yellow the polymer particles become colored.[25] This proves that swelling is highly cooperative in nature which means that not only the solvent is transported into the polymer particles but also the water-insoluble solute. It was experimentally proven by means of UV-microscopy that polystyrene particles take up poly(methyl methacrylate-*co*-pyrenemethacrylate).[15,26] This is quite surprising as both polymers are incompatible. Also, if the organic liquid is a non-solvent for the polymer spontaneous emulsification takes place. Additionally, another interesting effect was observed by means of ellipsometric light scattering (ELS).[27] Figure 8 displays data of the ellipsometric parameters $\tan(\Psi)$ (amplitude ratio) and Δ (phase shift) for the two samples (pure PS latex EUR63 and after contact with oct-1-ene) and the two available wavelengths of light (633 nm and 532 nm). The common shift in the minimum position of $\tan(\Psi)$ and the step in Δ clearly indicates a change in the particle structure. A fit of the ELS data is based on the Mie theory for the scattering of a coated sphere. For the pure sample, the data are reasonably described already by a homogenous sphere without coating. The core refractive index was kept fixed at the bulk refractive index of polystyrene $n_{PS} = 1.59$. The only fitting parameter is the core radius, where a value $R_{core} = 89.3$ nm is obtained. For the sample with oct-1-ene, three fits with different fixed parameters were performed. Table 1 lists the results and the obtained values for χ^2 as a measure of the fit quality.

The first fit keeps the core radius and refractive index of the sample without oct-1-ene. As a result, a layer with a thickness of 14 nm and a refractive index of 1.466 is obtained. The latter value exceeds significantly the refractive index of oct-1-ene. Therefore, this model of an un-swollen particle which is wetted by the alkene is not consistent. The second fit fixes the oct-1-ene refractive index as contrast for the shell and sticks to the polystyrene value as refractive index of the core. Here, a small increase in the core radius and a layer thickness of 14.6 nm are obtained. Finally, a model of a homogenous sphere with variable refractive index and radius was applied. As a result, the radius becomes slightly larger and the core refractive index slightly lower than before. This model corresponds to colloid particles homogeneously swollen with oct-1-ene. The value of χ^2 is significantly larger than for the other two fits, which indicates that this model is less suitable than the others. It should be

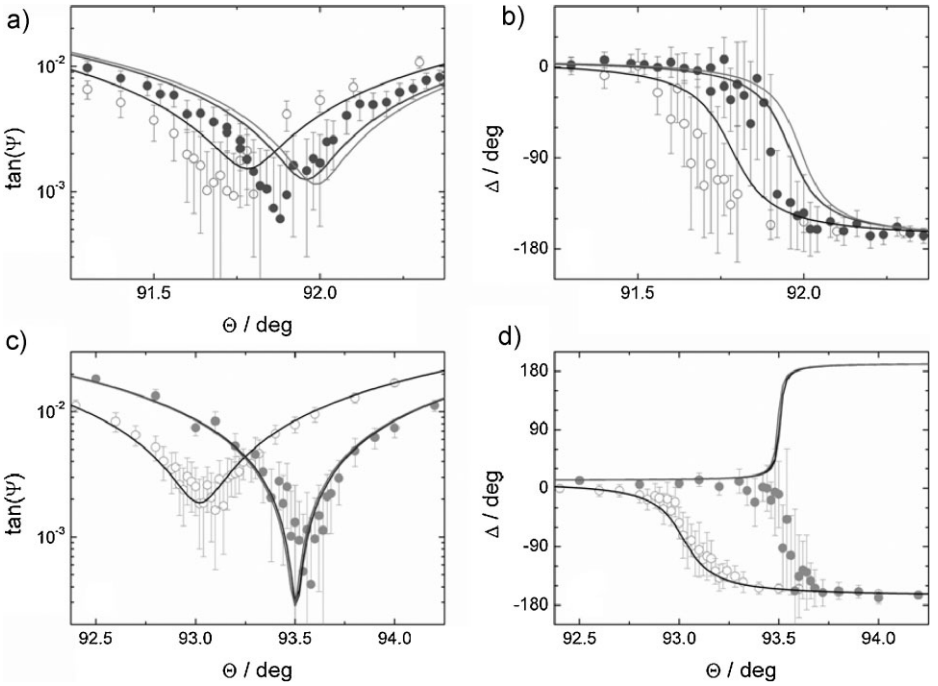

Figure 8.
Data for the ellipsometric parameters tan(Ψ) (a,c) and Δ (b,d) for a pure sample (○) and a sample with oct-1-en on the top (●), measured with light wavelength 633 nm (a,b) and 532 nm (c,d); lines mark the fits as described in the text.

mentioned further, that the data quality for the measurements with green light (wavelength 532 nm) is strongly reduced if the full power (400 m*W*) of the light source is applied to the samples. The data shown above are obtained with a strongly reduced power. The effect of light power and pressure fits better to a particle with loosely bound liquid shell (fit 2) than for a swollen colloid (fit 3). Therefore, an unswollen colloid wetted by oct-1-ene seems the most promising assumption. The deviations in Figure 8 between the fits and experimental data are probably due to optical anisotropy in the particles caused by stress birefringence. ELS has been shown to be very sensitive to anisotropy effects [28]. In Figure 8d the data show a $0 \rightarrow -180^\circ$ step, while the fit describes a $0 \rightarrow 180^\circ$ step. Note that $\Delta = -180^\circ$ and $\Delta = +180^\circ$ are equivalent, so only the data points in the transition really deviate from the fit. The wrong direction of the fit might be an effect of birefringence. As a cross-check, both samples were investigated by dynamic light scattering. Data for the apparent diffusion constant determined at several angles were extrapolated to $q^2 = 0$, where q is the modulus of the scattering vector. The extrapolation value was inserted to obtain the hydrodynamic radius R_h for the two samples. The result is $R_h = 91$ nm for the

Table 1.
Parameters obtained for different fits of the system PS particles/1-octene.

Fit	R_{core}/nm	n_{core}	d_{shell}/nm	n_{shell}	χ^2
1	89.3 (fix)	1.59 (fix)	13.9 ± 0.7	1.466 ± 0.003	192.9
2	92.2 ± 0.1	1.59 (fix)	14.6 ± 0.8	1.408 (fix)	188.15
3	98.0 ± 0.4	1.556 ± 0.002	–	–	262.93

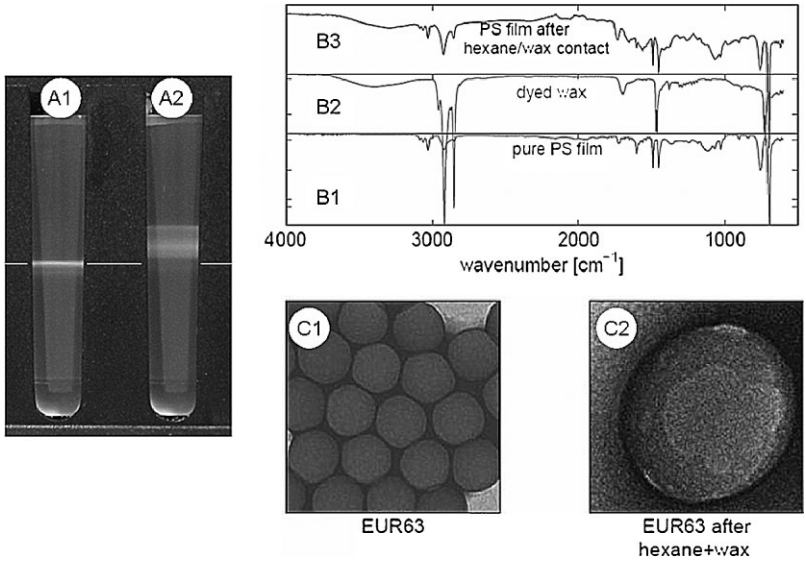

Figure 9.
Results proving the adsorption of hexane (A) and candle wax onto PS latex particles (B, C); A – ultracentrifugation in a sucrose density gradient, A1 – pure PS latex, A2 – PS + hexane; B – FT-IR spectroscopy, B1 – pure PS film, B2 – candle wax, B3 – film prepared from the PS latex phase after contact with candle wax in hexane solution; C – TEM, C1 – pure PS particles, C2 – PS particles covered with wax patches (lighter regions on the particles).

pure sample and $R_h = 99$ nm for the sample with oct-1-ene. These values fit well to the results deduced from ELS.

Also hexane as non-solvent forms a thin layer around the PS particles (images A of Figure 9). If a solution of candle wax in hexane is placed on the top of the PS latex the particles are coated with this solution and after evaporation of hexane with a thin wax layer as proven by FT-IR spectroscopy and TEM (images B and C of Figure 9).

The results of ultracentrifugation in a sucrose gradient and the FT-IR data clearly prove the interaction of PS latex particles with hexane and candle wax in hexane solution, respectively. Moreover, ELS with a CCD camera as detector prove the interaction of candle wax in hexane solution with PS latex particles.[29]

The last example proves the interaction of colloidal silica particles with a candle wax in hexane solution by TEM. The clarity of these results is quite surprising as the silica particles have a size of only about 15 nm.

The TEM images do not show any clearly visible difference in the appearance of pure and coated silica particles. But the enumeration of some 1200 particles reveals a size increase of the silica particles in contact with the candle wax in hexane solution of about 1 nm in the average particle diameters.

Conclusions

There are, besides the 'classical' way of encapsulation of preformed inorganic particles via emulsion polymerization, several other promising possibilities to synthesize inorganic – polymeric nanocomposites. These techniques take advantage of the newly discovered colloid - chemical effects in combination with special techniques of radical polymerization.

The synchronization of the nucleation of inorganic and polymeric particles is a good chance to control the morphology of the composite particles.

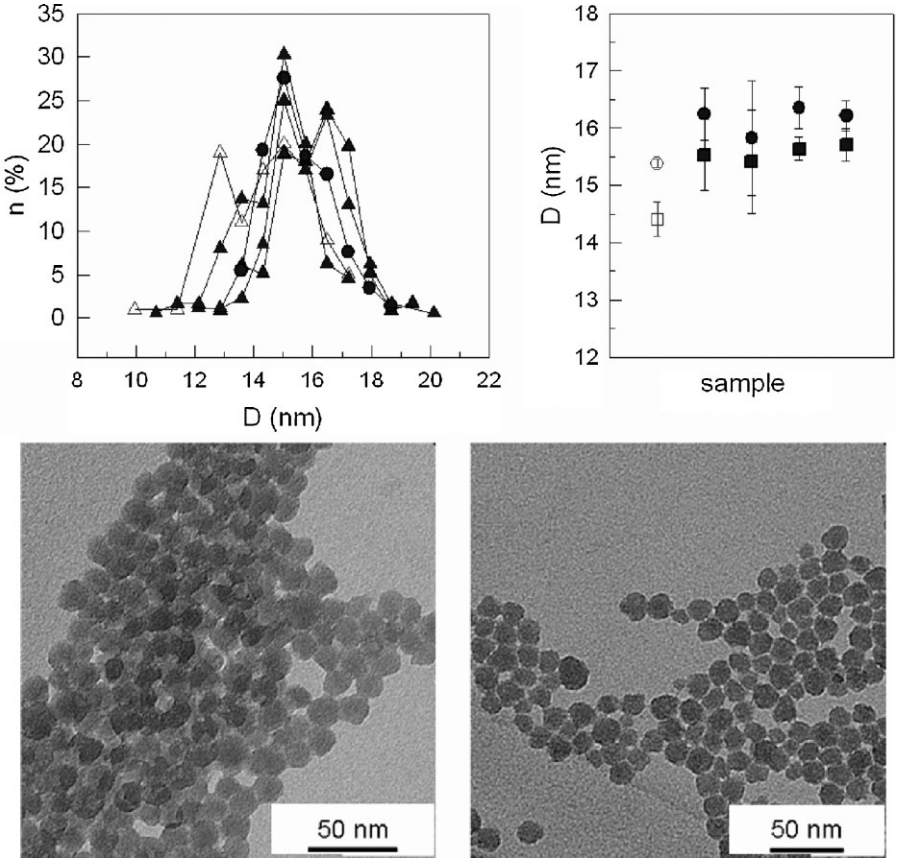

Figure 10.
TEM images of pure silica particles (lower left image) and silica particles after contact with a candle wax in hexane solution (lower right image); upper row - evaluation data (open symbols - pure silica particles, filled symbols - after contact with candle wax in hexane solution) of the enumeration of the TEM images regarding the particle size distribution (left graph) and the average diameter (filled circles - intensity average diameter, filled squares – number average diameter); the filled symbols represent 4 different samples.

The established strategy in synthesis of block copolymer particles via aqueous heterophase polymerization can be utilized to prepare silica containing block copolymer particles by joint polymerization where radical polymerization and hydrolytic condensation take place simultaneously. Calcination of these block-copolymer composite particles results in silica of different morphology. Depending on the composition of initial block-copolymer particles either silica nanoparticles or nanoporous silica materials are accessible.

Spontaneous emulsification is a very new modus operandi to obtain inorganic – polymeric nanocomposite particles starting from preformed materials. The two essential steps are the spontaneous formation of drops of an organic solution in contact with an aqueous dispersion and the interaction of both types of dispersed hydrophobic particles obviously driven by the aqueous environment.

[1] E. Bourgeat-Lami, E. Duguet, in: ''Functional Coatings'', **2006**, 85.
[2] E. Bourgeat-Lami, *Hybrid Mater.* **2007**, 87.
[3] H. Cölfen, M. Antonietti, *Metal Ions Life Sci.* **2008**, *4*, 607.
[4] A. Berman, *Metal Ions Life Sci.* **2008**, *4*, 167.

[5] M. Sumper, E. Brunner, *Chem. Bio. Chem.* **2008**, *9*, 1187.
[6] J. Watanabe, M. Akashi, *Bio-Inorg. Hybrid Nanomater.* **2008**, 193.
[7] S. H. Yu, H. Cölfen, K. Tauer, M. Antonietti, *Nature Mater.* **2005**, *4*, 51-U5.
[8] N. Nassif, N. Gehrke, N. Pinna, N. Shirshova, K. Tauer, M. Antonietti, H. Cölfen, *Angew. Chem. Int. Ed.* **2005**, *44*, 6004.
[9] K. Tauer, M. Antonietti, L. Rosengarten, H. Müller, *Macromol. Chem. Phys.* **1998**, *199*, 897.
[10] I. Kühn, K. Tauer, *Macromolecules* **1995**, *28*, 8122.
[11] K. Tauer, K. Padtberg, *AIP Conf. Proc.* **2000**, *534*, 432.
[12] K. Tauer, V. Khrenov, *Macromol. Symp.* **2002**, *179*, 27.
[13] P. Schuck, *Biophys. J.* **2000**, *78*, 1606.
[14] S. Nozari, Master thesis ''Joint Nucleation of Organic/Inorganic Nanoparticles'', MPI of Colloids and Interfaces, University of Potsdam, Golm/Potsdam, **2002**.
[15] K. Tauer, H. Hernandez, S. Kozempel, O. Lazareva, P. Nazaran, *Coll. Polym. Sci.* **2008**, *286*, 499.
[16] K. Padtberg, PhD thesis ''On-line Verfolgung von Nukleierungsprozessen'', MPI of Colloids and Interfaces, University of Potsdam, Golm/Potsdam, Germany, **2001**.
[17] K. Tauer, V. Khrenov, N. Shirshova, N. Nassif, *Macromol. Symp.* **2005**, *226*, 187.
[18] M. D. C. Topp, I. H. Leunen, P. J. Dijkstra, K. Tauer, C. Schellenberg, J. Feijen, *Macromolecules* **2000**, *33*, 4986.
[19] K. Tauer, M. Mukhamedjanova, C. Holtze, P. Nazaran, J. Lee, *Macromol. Symp.* **2007**, *248*, 227.
[20] L. C. Dong, A. S. Hoffman, *J. Contr. Rel.* **1990**, *13*, 21.
[21] K. Tauer, D. Gau, S. Schulze, A. Völkel, publication in prep.
[22] If PSS is used as precursor polymer the solid contains after calcination also some sodium sulphate which can easily be removed by washing with water.
[23] K. Tauer, S. Kozempel, G. Rother, *J. Coll. Interf. Sci.* **2007**, *312*, 432.
[24] S. Kozempel, K. Tauer, G. Rother, *Polymer* **2005**, *46*, 1169.
[25] K. Tauer, S. Nozari, A. M. I. Ali, S. Kozempel, *Macromol. Rapid Commun.* **2005**, *26*, 1228.
[26] K. Tauer, H. F. Hernandez, S. Kozempel, O. Lazareva, P. Nazaran, *Macromol. Symp.* **2007**, *259*, 253.
[27] A. Erbe, K. Tauer, R. Sigel, *Phys. Rev. E* **2006**, *73*.
[28] A. Erbe, R. Sigel, *Eur. Phys. J. E* **2007**, *22*, 303.
[29] A. Stark, PhD thesis ''CCD Based Ellipsometric Light Scattering'', MPI Colloids and Interfaces, University of Potsdam, Golm/Potsdam, Germany, **2008**.

